applied sciences

MDPI

Article

Controlling Chemical Reactions in Confined Environments: Water Dissociation in MOF-74

Erika M. A. Fuentes-Fernandez [1,†], Stephanie Jensen [2,†], Kui Tan [1], Sebastian Zuluaga [2], Hao Wang [3], Jing Li [3], Timo Thonhauser [2,4] and Yves J. Chabal [1,*]

1 Department of Materials Science and Engineering, University of Texas at Dallas, Richardson, TX 75080, USA; erika.fuentesf@gmail.com (E.M.A.F.-F.); kuitan@utdallas.edu (K.T.)
2 Department of Physics and Center for Functional Materials, Wake Forest University, Winston-Salem, NC 27109, USA; jensensj@wfu.edu (S.J.); sebastian.zuluaga@vanderbilt.edu (S.Z.); thonhauser@wfu.edu (T.T.)
3 Department of Chemistry and Chemical Biology, Rutgers University, Piscataway, NJ 08854, USA; whwhuccms@gmail.com (H.W.); jingli@rutgers.edu (J.L.)
4 Department of Chemistry, Massachusetts Institute of Technology, Cambridge, MA 02139, USA
* Correspondence: chabal@utdallas.edu; Tel.: +1-972-883-5751
† These authors contributed equally to this work.

Received: 5 January 2018; Accepted: 1 February 2018; Published: 12 February 2018

Abstract: The confined porous environment of metal organic frameworks (MOFs) is an attractive system for studying reaction mechanisms. Compared to flat oxide surfaces, MOFs have the key advantage that they exhibit a well-defined structure and present significantly fewer challenges in experimental characterization. As an example of an important reaction, we study here the dissociation of water—which plays a critical role in biology, chemistry, and materials science—in MOFs and show how the knowledge of the structure in this confined environment allows for an unprecedented level of understanding and control. In particular, combining in-situ infrared spectroscopy and first-principles calculations, we show that the water dissociation reaction can be selectively controlled inside Zn-MOF-74 by alcohol, through both chemical and physical interactions. Methanol is observed to speed up water dissociation by 25% to 100%, depending on the alcohol partial pressure. On the other hand, co-adsorption of isopropanol reduces the speed of the water reaction, due mostly to steric interactions. In addition, we also investigate the stability of the product state after the water dissociation has occurred and find that the presence of additional water significantly stabilizes the dissociated state. Our results show that precise control of reactions within nano-porous materials is possible, opening the way for advances in fields ranging from catalysis to electrochemistry and sensors.

Keywords: metal organic framework; reaction mechanism; confined environment

1. Introduction

The assembly of water at the interface of materials has become one of the central topics in biology, chemistry, and materials sciences [1]. It can lead to catalytic reactions at oxide surfaces [2–4] and has also attracted considerable interest due to promising applications in photocatalysis, electrochemistry, and sensors [5–8]. Although understanding the mechanism of water dissociation at surfaces is of paramount interest, its study on flat oxide surfaces is unfortunately highly non-trivial—mostly due to experimental challenges in structural characterization and high pressure required (on the order of 20 atm) for in-situ studies on flat surfaces [1,7,9–12]. In this respect, metal organic frameworks (MOFs) are attractive systems to study reactions since they are well-controlled crystalline environments with well-defined metal oxide centers [3,4,13,14], in which high gas densities can be achieved at relatively

low external pressures. MOFs are networks of metal ions linked by organic ligands, forming a well-characterized cross-linked structure. Due to their porous nature, gas molecules can penetrate deeply into the MOF network [15] and experience adsorption forces that allow for significantly longer residence times than at surfaces under similar pressures and temperatures, thus fostering an environment much more conducive to trigger, observe, and study desired reactions.

MOFs are already well studied for their high surface areas and nano-porous structure as they provide an ideal environment for many applications ranging from gas storage and separation to sensors and catalysis [16–20]. Amongst the vast amount of existing MOFs, MOF-74 is of great interest since it contains a high density of coordinately unsaturated metal centers (also called open metal sites) in metal-oxide pyramid clusters, which act as active adsorption sites for many small molecules such as H_2, CO, CO_2, NO, CH_4, and H_2O [21–29]. In particular, Zn-MOF-74 exhibits a strong affinity to water, making it ideal for examining various water reaction mechanisms [30]. We have already studied the reaction of water molecules alone in Zn-MOF-74 [2,3,14,31], finding direct evidence for water dissociation at only 150 °C—this was achieved through the use of D_2O instead of H_2O, observing a clear fingerprint peak at 970 cm^{-1} that corresponds to a O–D bending vibration of OD groups formed upon deuteration of the organic linker [3]. The concerted action between open metal sites and linker phenolate group plays an essential role in breaking up water molecules since water molecule establish strong coordinative bond with metal center via its oxygen and hydrogen bonding interaction with nearby –C–O– moiety from organic linker. With an increase in temperature the water molecule dissociates into D and OD [3]. The OD binds to the open metal sites, while the D atom is transferred to the oxygen of phenolate group. The reaction with water (H_2O) itself follows of course the same dissociation pathway, but the spectroscopic signature is impossible to detect with H_2O as hydrogen blue shifts the peak outside the phonon gap of the MOF, where it strongly couples to many other modes. It was also demonstrated that the formation of water networks within the MOF pores was crucial to further lower the corresponding reaction barrier via a proton-exchange mechanism and that physical obstruction of this network with inert molecules (He, Ar) hinders the reaction [14].

In the present work, we explore the role of co-adsorbed alcohol molecules and present a kinetic analysis of the water dissociation reaction inside Zn-MOF-74 in the presence of additional guest molecules. We find that alcohol molecules affect the dissociation rate, either by enhancing or blocking the reaction depending on the type of interaction resulting from such co-adsorption. Specifically, methanol enhances the reaction due to H-bonding interactions, while isopropyl alcohol (IPA) hinders it because steric interactions dominate in that case. The knowledge derived from these combined studies is directly relevant to fields such as catalysis and sensors by providing a means to control water-related reactions, as well as to applications such as gas storage and separation by suppressing water dissociation and therefore extending the MOF lifetime.

2. Methods

2.1. Sample Preparation and In-Situ Infrared Spectroscopy

Zn-MOF-74 powder (1.5 mg) was gently pressed onto a KBr pellet and placed inside a high-pressure cell (Specac Ltd., Orpington, UK; product number P/N 5850c). This high-pressure cell was located in the sample compartment of a Nicolet 6700 FTIR spectrometer (Thermo Scientific Inc., Mountain View, CA, USA) with the sample at the focal point of the beam. All the infrared (IR) spectroscopic data were collected with a liquid N_2-cooled mercury cadmium telluride (MCT-B or MCT-A from Thermo Scientific Inc., Mountain View, CA, USA) detector. The cell was connected to different gas lines for exposure and a vacuum line for evacuation. All spectra were recorded in transmission mode from 400 cm^{-1} (MCT-B) or 650 cm^{-1} (MCT-A) to 4000 cm^{-1} (4 cm^{-1} spectral resolution). Regular water (H_2O) and heavy water (D_2O) were used, with most of the work performed with D_2O to avoid a MOF phonon overlap in the spectral range of the O–H bending vibration [2,3].

2.2. Experimental Measurement Conditions

Once inside the high-pressure cell, the MOF powder was activated by annealing at 180 °C for at least 4 h in vacuum (<50 mTorr) to remove the solvent and ambient humidity from the inside of MOF's pores. The sample was then cooled down to room temperature. In a mixing gas chamber connected to the high-pressure cell (where the sample is located). 8 Torr of alcohol (methanol or isopropyl alcohol) was prepared with 8 Torr of deuterated water (D_2O). The alcohol/D_2O mixture was then introduced into the main chamber and allowed to stabilize for 10 min, after which the temperature was raised to 180 °C. Spectra were recorded as a function of time until stabilization of the 970 cm^{-1} peak was reached (~8 h). For completeness, the results are compared to data previously reported by our group using He and pure D_2O [14]. Measurements with pure MeOH and its deuterated analog (MeOD) are also presented as reference in the Supplementary Information (See Figure S2).

2.3. Computational Details

Ab initio modeling was performed at the density functional theory (DFT) level in Vienna Ab initio simulation package (VASP) [32,33]. To include van der Waals interactions of guest molecules within the MOF, the exchange-correlation functional vdW-DF was used [34–37]. The energy cutoff was set to 600 eV and only the Γ point was considered due to the size of the system. The 54 atom rhombohedral primitive cell of Zn-MOF-74 was first relaxed until the forces on the atoms were below 1 meV/Å. Binding energies were then calculated for MeOH, H_2O, OH, and H (and deuterated equivalents), with the hydrogen or deuterium at the metal center and on the oxygen atom of the MOF organic linker. After the guest molecules were placed into the MOF, each structure was again relaxed until the forces on all atoms were below 1 meV/Å. Reaction barriers were calculated with a standard transition-state search algorithm, i.e., the nudged-elastic band method [38,39], as implemented in VASP.

3. Results and Discussion

3.1. Experimental Quantification of the Water Dissociation Reaction Rate

To determine the impact of guest molecules on the water dissociation rate through chemical interactions, we studied this reaction in the presence of alcohol molecules inside the MOF as a function of temperature and time. After MOF activation, the alcohol/D_2O mixture was introduced into the cell at room temperature and IR absorption spectra were subsequently recorded with the sample at 180 °C, monitoring the above-mentioned O–D bending vibration at ~970 cm^{-1}, which is the product of the D_2O dissociation [3]. The IR spectra were recorded until the intensity of the 970 cm^{-1} peak stabilized. In this manner, the kinetics of methanol/D_2O and isopropanol/D_2O mixtures could be compared for different alcohol pressures with previously reported data with either pure D_2O or inert gas/D_2O mixtures [14], using the integrated area of the 970 cm^{-1} peak as a quantification of D_2O dissociation. Results with pure methanol and pure deuterated methanol are also presented for comparison in the supplementary information (see Figure S2).

Figure 1a shows the representative water dissociation fingerprint at 970 cm^{-1} after 8 h of reaction at 180 °C for the different mixtures analyzed inside the MOF, which is sufficient time for the reaction to stabilize in all environments. All spectra are normalized to the quantity (weight) of the MOF powder. The feature at 1003 cm^{-1}, only observed for the mixture with 8 Torr MeOH, will be discussed shortly. Figure 1b shows the kinetic evolution of the tested reactions. It is clear that water dissociation rates strongly depend on the environment: the $D_2O \rightarrow 2D + O$ reaction is faster in the presence of methanol and slower in the presence of isopropanol or inert gases such as He. Experimentally, we find that the water reaction rates inside MOF-74 are fastest to slowest as follows: 8 Torr MeOH > 4 Torr MeOH > Pure D_2O > 8 Torr IPA > 950 Torr He. Table 1 reports the percent of dissociated water molecules, as compared with pure water (100%), as function of guest molecules. These data can be used to examine the dependence on the alcohol pressure, for instance in the case of methanol. The dependence is clearly not linear, but can be well fitted with a quadratic fit, $y = 25.5x^2 - 149.5x + 219$, where y is the percent

dissociation and x the pressure, pointing to the importance of the local environment. Indeed, water dissociation is faster when there are more MeOH molecules inside the MOF pore, i.e., when a network can be formed.

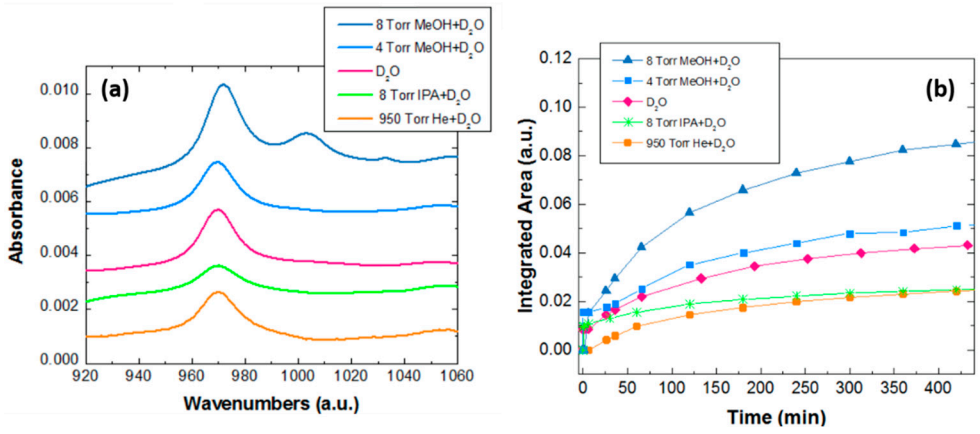

Figure 1. (**a**) Infrared spectra of Zn-MOF-74 impregnated with the different alcohol mixtures (methanol = Me and Isopropyl alcohol = IPA) for 8 h at 180 °C, compared to a He/D_2O mix and pure D_2O previously reported [14]. (**b**) Kinetic plots of the dissociation reaction over time (integrated area of 970 cm^{-1} band). All spectra are normalized to metal organic frameworks (MOF) quantity.

Table 1. Percentage of deuterated water dissociated after 8 h of reaction for D_2O + guest molecules, based on data shown in Figure 1b, compared to pure D_2O (taken as the reference, i.e., 100%).

D_2O + Guest Molecules	Percentage of D_2O Dissociated after 8 h (%)
8 Torr D_2O	100
4 Torr MeOH + 8 Torr D_2O	122
8Torr MeOH + 8 Torr D_2O	195
8 Torr IPA + 8 Torr D_2O	61
950 Torr He + 8 Torr D_2O	61

Methanol is interesting, namely because of its small size that minimizes steric hindrance within the MOF pore. Different pressures of methanol were tested while keeping the D_2O pressure at 8 Torr for all experiments. The infrared spectra measured after introduction of a MeOH/D_2O mixture as a function of temperature and time are presented in Figure 2. After introducing a methanol/D_2O mixture into Zn-MOF-74 at room temperature, the C–O stretch mode of methanol gas phase was observed at 1033 cm^{-1} (see Figure S3). As the temperature increases, this band red-shifts to 1010 cm^{-1} at 170 °C and to 1003 cm^{-1} at 180 °C, which suggests a strong interaction of methanol with the MOF metal center [40].

Water dissociation only proceeds at 180 °C, as evidenced by the appearance of the 970 cm^{-1} peak. At that point, the peak at 1003 cm^{-1} weakens, indicating that C–O dissociation occurs. The synergistic dissociation of methanol and D_2O results in a faster D_2O dissociation reaction. In fact, the increased dissociation with MeOH pressure described earlier suggests that the presence of methanol fosters the reaction, mediated by the metal site, almost doubling the reaction yield in 8 Torr MeOH. This observation can be rationalized with first-principles calculations as detailed next.

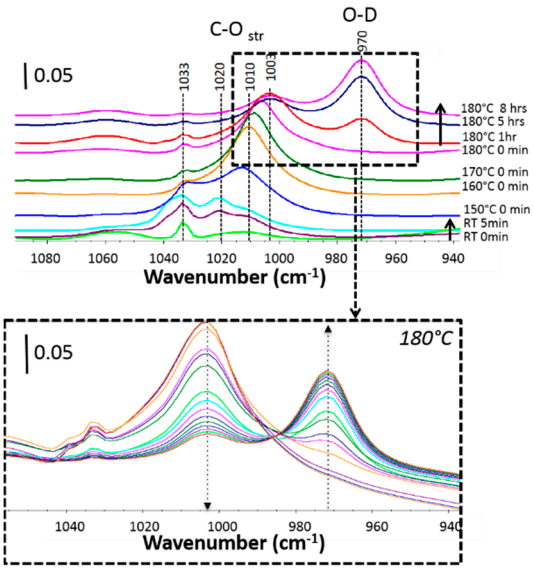

Figure 2. (**Top**) Absorbance IR absorption spectra of Zn-MOF-74 loaded with a mixture of 8 Torr methanol and 8 Torr D_2O as a function of temperature and time. (**Bottom**) Detailed reaction evolution at 180 °C from 0 to 8 h (dashed arrows indicate the time evolution).

3.2. Theoretical Analysis of the Water Dissociation Reaction Rate

Calculations summarized in Table 2 show that, when both water and methanol are present in the system, methanol associates to the metal center and water binds to the organic linker. Water alone can associate with both the metal linker and organic linker almost equally, but the MeOH has a stronger binding (association) to the metal center than water. In fact, MeOH does not interact with the oxygen atom of the linker, in contrast to water. Consequently, the OH group of MeOH binds to the metal center upon cooperative adsorption of MeOH and D_2O, while the D atom from water binds to the oxygen atom of the linker since the metal site is occupied, and the OD part of D_2O binds to the CH_3 group of MeOH, as illustrated in Figure 3a. The dissociation reaction then proceeds as follows: First, there is a lengthening and thus weakening of the C–O bond in MeOH, which is in agreement with the observed redshift of ν(C–O) from 1033 cm^{-1} to 1003 cm^{-1} and facilitates subsequent OH exchange. Indeed, at the transition state, the OD group from the neighboring D_2O molecule approaches the methyl group, while the other D atom bonds to the oxygen of the ligand. As OH (from methanol) bonds to the Zn center very strongly (see Table 2) and D (from D_2O) binds strongly to O (see Table 2), the OD group is transferred to the methyl group to complete the hydroxyl exchange on the methyl group. While such an exchange is not common, the strong energetic gain drives this reaction. As MeOD is formed, a single D remains at the oxygen of the linker, characterized by the well-studied 970 cm^{-1} IR fingerprint [3]. Note that in this cooperative reaction the energy barrier for dissociation is also reduced by a clustering effect [14]. The products of the dissociation reaction (OH on the Zn^{2+} site or D on oxygen site) bind much more strongly than the initial reactants (H_2O/D_2O and MeOH) that are only bound through weaker van der Waals interactions, as shown in Table 2.

Table 2. Calculated binding energies (in eV) of reactants and products to both the Zn metal center and the organic linker prior to and after water dissociation for a methanol/water mixture. DNB indicates that the functional did not bind.

Binding Energies of Reactant and Products Inside Zn-MOF-74		
Functional	Zn Metal Center E_b (eV)	Organic Linker E_b (eV)
MeOH	−0.780	DNB
H_2O	−0.612	−0.610
OH	−2.442	DNB
H	−2.002	−1.932

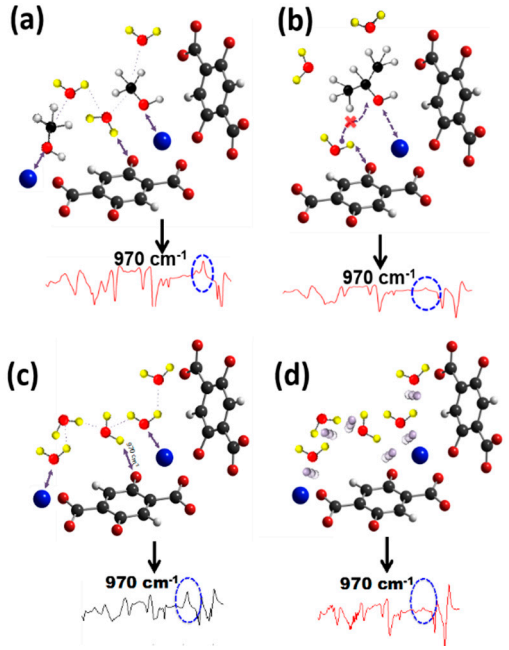

Figure 3. Schematic of Zn-MOF-74 interacting with (**a**) methanol/D_2O assisting the reaction by the formation of clusters in a similar fashion as pure D_2O; (**b**) isopropanol/D_2O hindering the interaction of D_2O with the secondary carbon in the IPA molecule due to the steric barrier; (**c**) pure deuterated water (D_2O) and cluster formation; and (**d**) He/D_2O, with He obstructing water cluster formation. White, yellow, red black, blue and purple spheres represent H, D, O, C, Zn, and He atoms. Each schematic has a normalized Zn-MOF-74 IR spectra after 8 h of reaction at 180 °C.

The mechanism by which MeOH can thus speed up the reaction is as follows: When water dissociates without any other guest molecules present, it is the water molecule bound to the metal center that dissociates, as shown in Figure 3c [3,14,30,31]. In the presence of MeOH, this pathway is blocked, as MeOH takes the place on the metal site, which forces the water bound to the linker, as shown in Figure 3a. The weakening of C–O bond in MeOH, evidenced by the frequency shift, is even more pronounce when an OD group (from D_2O) is in close proximity, which makes MeOH an effective precursor for D_2O dissociation, leading to D bonding to the oxygen linker, with reformation of a methanol (MeOD) molecule. To further support the experimental observation of a faster reaction, the vibrational modes of the D_2O/MeOH system were also calculated in conjunction with Zn-MOF-74 and characterized using J-ICE [41]. After applying a systematic scaling of 7% to all computed frequencies, a peak at 1030 cm^{-1} was found for the C–O stretching mode of gas-phase MeOH; that mode was also calculated to red-shift to 1005 cm^{-1} upon adsorption in the MOF at the Zn metal centers and interaction with D_2O. This calculated 25 cm^{-1} red shift is in excellent agreement with the measured 30 cm^{-1} redshift, i.e., from 1033 cm^{-1} to 1003 cm^{-1}, mentioned above. As pointed out, this red-shift is indicative of the C–O bond weakening, which is a requirement for hydroxyl

exchange MeOH → MeOD. The disappearance of the 1003 cm^{-1} mode in Figure 2b thus indicates that more and more MeOH gets converted into MeOD (1060 cm^{-1}) via the mechanism discussed above.

Isopropyl alcohol, on the other hand, slows down the dissociation reaction over time (Figure 1b), similarly to what is observed for the He/D_2O mixture (Figure 3d), suggesting that steric interactions are important in the case of IPA. We previously reported that inert gases such as He and Ar block the intermolecular interactions between water molecules by disrupting the formation of water clusters (networks), thus effectively increasing the reaction barrier [14]. Similarly to noble gases, IPA prevents water cluster formation, even at much lower pressure than noble gases, thus slowing down the dissociation rate. In contrast to methanol that fosters the reaction, the size of IPA prevents reaction more than the propensity of its OH group to react with the metal site, as discussed below. Note that the chemical and crystalline structures of MOF-74 remain after D_2O/alcohol exposure (see Figure S7).

In summary, the experimental results supported by computational analysis suggest the reactions illustrated in Figure 3 (with reaction pathways simulated for 1 vs. 4 water molecules reacting with 1 MeOH molecule is presented in Supplementary Materials in Section S4). Methanol by itself has a higher steric hindrance than water, but not high enough to block the reaction given the overall pore size in MOF-74. Because the reaction is experimentally observed to take place at high temperature, dissociation of methanol is favored; as a consequence of MeOH's stronger interaction with the metal center, the reaction achieves a more stable final state (Table 2). After interacting with the metal center, MeOH and D_2O molecules form an organized structure (cluster), which helps to reduce the dissociation reaction barrier of D_2O at the organic linker—and the reaction proceeds as outlined above. Steric obstruction of water clustering due to a bulkier alcohol, such as isopropanol, is presented in Figure 3b. The $-CH_3$ groups surrounding the secondary carbon block water molecules from clustering and reduce the dissociation rate by 40% in comparison to pure D_2O as presented in Table 1. Note that a lower pressure (8 Torr) of IPA is needed than He gas (950 Torr) to reduce the water dissociation rate to the same level, suggesting co-adsorbing IPA is an effective way to suppress water dissociation and therefore to increase the MOF stability for gas uptake and other applications. Further details are presented in the supplementary information in Section S5.

Comparing the two pathways that obstruct the reaction, a schematic of the reaction mechanism of IPA/water is presented in Figure 3b. The IPA blocks the reaction by its interaction with the metal center, requiring a lower pressure to occupy all metal centers in the unit cell [42]. On the contrary He/water reaction mechanism presented in Figure 3d illustrates how adding guest molecules physically prevent the formation of organized water clusters, hence reducing water dissociation reaction at higher pressures. Thus, the water dissociation reaction can be simply controlled by assisting or hampering cluster formation by a guest molecule such as methanol or isopropanol, therefore systematically tuning the effective reaction barriers [14].

For both pure water and alcohol/water mixtures, a central aspect of MOF-74 is the ability to adsorb several molecules within each pore at relatively low external pressures (~few Torr), thanks to van der Waals attractive forces. This is only possible in the confined space of a nanoporous material. In the confined environment of MOF-74, several water and alcohol molecules can coexist within each pore, forming nano-structures, which generally lowers the dissociation barriers and stabilizes the dissociated state. Consequently, the formation of water or alcohol/water networks occurs at convenient pressures, and these networks can remain stable even after the cell is pumped out. Such networks cannot be realized on flat oxide surfaces because the external pressure would need to be prohibitively high and because entropy would prevent structured networks to develop for lack of a supporting nanostructured framework around [11,12].

3.3. Stabilization Effect of Additional Water on the Water Dissociation Reaction

A final point needs to be addressed, i.e., the stability of the dissociation products, because the reverse reaction barriers tend to be low. A quantitative analysis is difficult because reaction barriers are difficult to evaluate in systems where there may be several reaction pathways. Nonetheless,

we have attempted such analysis by calculating the water dissociation reaction barrier using a standard transition-state search algorithm [38,39], in the presence of a varying amount of additional water molecules. In particular, we investigate the reaction mechanism involving MeOH assistance as discussed above, and compare that with the dissociation of pure H_2O found previously [14]. Results are presented in Table 3 and Figure 4.

Table 3. Reaction barriers for the MeOH assisted and pure H_2O dissociation in the presence of varying amounts of additional water molecules.

Water Systems	No. H_2O	Initial State (eV)	Transition State (eV)	Final State (eV)	Forward Barrier (eV)	Backward Barrier (eV)
MeOH + H_2O	1	0	1.607	1.386	1.607	0.220
	4	0	0.932	0.598	0.932	0.333
H_2O	1	0	1.085	1.054	1.085	0.031
	2	0	0.964	0.832	0.964	0.132
	3	0	0.990	0.571	0.990	0.418
	4	0	0.688	0.530	0.688	0.158
	5	0	0.690	0.580	0.690	0.110

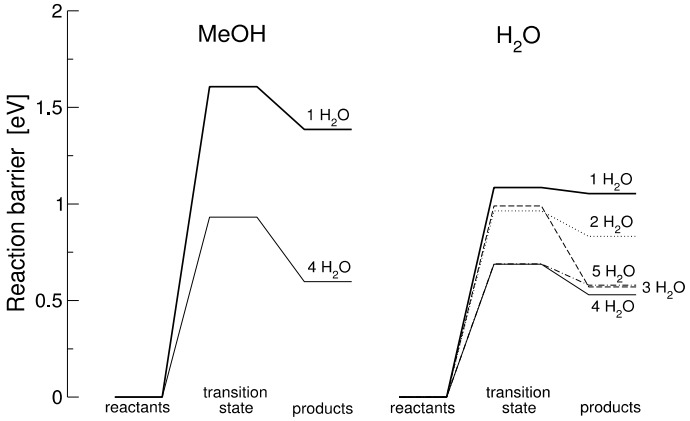

Figure 4. Reaction barriers for the MeOH assisted and pure H_2O dissociation in the presence of varying amounts of additional water molecules.

In both cases—the MeOH assisted and pure H_2O dissociation—it is obvious that increasing the number of water molecules decreases the forward reaction barrier for the individual reactions. This behavior has been analyzed in detail for the H_2O case, where it was found that small water clusters form and are, in turn, responsible for decreasing the barrier [14]; we propose a similar mechanism in the presence of MeOH. However, more importantly, increasing the number of water molecules also increases the backward barrier, i.e., the barrier for the reverse reaction. In fact, in some cases (such as the pure water dissociation with only one H_2O) the reverse barrier is so low that the product state cannot be considered stable at all and, even at low temperature, will recombine back into water molecules. It is thus the presence of additional water molecules that stabilizes the product state and makes the reaction observable. Note that experimentally, it is very difficult to determine the exact amount of water molecules inside the MOF pore and nearby the reaction site, but it is estimated based on isotherm measurements corrected to the higher temperature (180 °C), that 8 Torr of water result in at least 6 to 8 water molecules in the MOF unit cell (calculations based on the ideal gas law) [42].

In the previous section, comparison between pure water and water/alcohol mixtures was based on total energy calculations, providing good support for experimental observations. Calculating reaction barriers through transition-state searches becomes increasingly more complex in the presence of more water molecules (due to the vastly growing space of possible arrangements and reaction pathways) so that such calculations only provide upper limits for reaction barriers. Due to their

complexity and computer time needed, we only investigated a limited set. For instance, barriers for a MeOH/water mixture are only calculated for one and four water molecules. Based on calculations presented in Figure 4, it is suggested that water dissociation does not proceed with only one water molecule. It appears that, in the case of MeOH the forward barrier is too high to account for the experimentally observed reaction at 180 °C; also, in the case of a single H_2O molecule, the backward barrier is so small that it would not be possible to observe the reaction before it reverses. In the H_2O case, the largest backwards barrier (0.418 eV) is found for three water molecules, but that scenario does not have the smallest forward barrier. While details are difficult to model and quantify, the results suggest that the presence of a small network of water molecules lowers the forward reaction, and the presence of water molecules remaining after the reaction stabilizes the products. In reality, there must be a dynamic equilibrium that gets established for given pressures. Therefore, this section only provides a suggestion for the mechanisms involved yet cannot unambiguously quantify them.

4. Conclusions

Combining in-situ infrared spectroscopic studies and first-principles DFT calculations, we have shown that the dissociation reaction of water molecules within MOF-74 can be controlled by co-adsorption of alcohols, just as it is hindered by inert gases. Bulky alcohol molecules such as IPA prevent water clustering, thus reducing water dissociation rates more effectively than inert gases at comparable external pressures. On the other hand, small alcohol molecules with a low boiling point, such as methanol, effectively accelerate water dissociation, without sterically hindering the process. In the confined environment of MOF-74, several water molecules can coexist within each pore, forming nano-structures, which generally lowers the dissociation barriers and stabilizes the dissociated state at low pressures. These results offer a potential approach to controlling water dissociation inside MOF-74, which is important for gas storage and separation applications. Since water is present in most biological, catalytic, and daily life applications, the understanding derived here provides new insight into the possibility of controlling water dissociation rates, which in turn affords a novel means for tuning chemical reactions in general.

Supplementary Materials: The following are available online at www.mdpi.com/2076-3417/8/2/270/s1. Sample preparation and activation methods; Powder X-ray diffraction pattern of Zn-MOF-74 sample; Isotherm measurement of N_2 adsorption into Zn-MOF-74; IR spectra of pure methanol (MeOH) and deuterated methanol (MeOD) interaction with Zn-MOF-74; Water dissociation reaction pathway in the presence of one and four water molecules; IR spectra of isopropanol (IPA) and D_2O interaction with Zn-MOF-74. This material is available free of charge at http://pubs.acs.org.

Acknowledgments: This work was entirely supported by the Department of Energy Grant No. DE-FG02-08ER46491. T.T. also acknowledges generous support from the Simons Foundation through Grant No. 391888, which endowed his sabbatical leave at MIT.

Author Contributions: H.W. and J.L. synthesized and characterized Zn-MOF-74 used in this work; E.M.A.F.-F., K.T. and Y.J.C. conceived, designed and perform the experimental part of the paper; S.J., S.Z. and T.T. performed the theoretical analysis. All authors contributed to the writing, and analysis of this paper.

Conflicts of Interest: The authors declare no conflict of interest.

References

1. Henderson, M.A. The interaction of water with solid surfaces: Fundamental aspects revisited. *Surf. Sci. Rep.* **2002**, *46*, 1–308. [CrossRef]
2. Tan, K.; Nijem, N.; Gao, Y.; Zuluaga, S.; Li, J.; Thonhauser, T.; Chabal, Y.J. Water interactions in metal organic frameworks. *CrystEngComm* **2015**, *17*, 247–260. [CrossRef]
3. Tan, K.; Zuluaga, S.; Gong, Q.; Canepa, P.; Wang, H.; Li, J.; Chabal, Y.J.; Thonhauser, T. Water Reaction Mechanism in Metal Organic Frameworks with Coordinatively Unsaturated Metal Ions: MOF-74. *Chem. Mater.* **2014**, *26*, 6886–6895. [CrossRef]
4. Ward, M.D. Confined systems: The bright side of MOFs. *Nat. Chem.* **2010**, *2*, 610–611. [CrossRef] [PubMed]
5. Hass, K.C.; Schneider, W.F.; Curioni, A.; Andreoni, W. The Chemistry of Water on Alumina Surfaces: Reaction Dynamics from First Principles. *Science* **1998**, *282*, 265–268. [CrossRef] [PubMed]

6. Brown, G.E., Jr. How Minerals React with Water. *Science* **2001**, *294*, 67–69. [CrossRef] [PubMed]
7. Bikondoa, O.; Pang, C.L.; Ithnin, R.; Muryn, C.A.; Onishi, H.; Thornton, G. Imaging water dissociation on TiO_2(110). *Nat. Mater.* **2006**, *5*, 189–192. [CrossRef]
8. Song, Z.; Fan, J.; Xu, H. Strain-induced water dissociation on supported ultrathin oxide films. *Sci. Rep.* **2016**, *6*, 22853–22858. [CrossRef] [PubMed]
9. Giordano, L.; Goniakowski, J.; Suzanne, J. Partial Dissociation of Water Molecules in the (3 × 2) Water Monolayer Deposited on the MgO (100) Surface. *Phys. Rev. Lett.* **1998**, *81*, 1271–1273. [CrossRef]
10. Odelius, M. Mixed Molecular and Dissociative Water Adsorption on MgO[100]. *Phys. Rev. Lett.* **1999**, *82*, 3919–3922. [CrossRef]
11. Carrasco, J.; Hodgson, A.; Michaelides, A. A molecular perspective of water at metal interfaces. *Nat. Mater.* **2012**, *11*, 667–674. [CrossRef] [PubMed]
12. Rodriguez, J.; Goodman, D.W. High-pressure catalytic reactions over single-crystal metal surfaces. *Surf. Sci. Rep.* **1991**, *14*, 1–107. [CrossRef]
13. Tan, K.; Canepa, P.; Gong, Q.; Liu, J.; Johnson, D.H.; Dyevoich, A.; Thallapally, P.K.; Thonhauser, T.; Li, J.; Chabal, Y.J. Mechanism of Preferential Adsorption of SO_2 into Two Microporous Paddle Wheel Frameworks $M(bdc)(ted)_{0.5}$. *Chem. Mater.* **2013**, *25*, 4653–4662. [CrossRef]
14. Zuluaga, S.; Fuentes-Fernandez, E.M.; Tan, K.; Li, J.; Chabal, Y.J.; Thonhauser, T. Cluster assisted water dissociation mechanism in MOF-74 and controlling it using helium. *J. Mater. Chem. A* **2016**, *4*, 11524–11530. [CrossRef]
15. Canepa, P.; Nijem, N.; Chabal, Y.J.; Thonhauser, T. Diffusion of Small Molecules in Metal Organic Framework Materials. *Phys. Rev. Lett.* **2013**, *110*, 026102. [CrossRef] [PubMed]
16. Suh, M.P.; Park, H.J.; Prasad, T.K.; Lim, D.-W. Hydrogen Storage in Metal–Organic Frameworks. *Chem. Rev.* **2011**, *112*, 782–835. [CrossRef] [PubMed]
17. Sumida, K.; Rogow, D.L.; Mason, J.A.; McDonald, T.M.; Bloch, E.D.; Herm, Z.R.; Bae, T.-H.; Long, J.R. Carbon Dioxide Capture in Metal–Organic Frameworks. *Chem. Rev.* **2011**, *112*, 724–781. [CrossRef] [PubMed]
18. Li, J.-R.; Sculley, J.; Zhou, H.-C. Metal–Organic Frameworks for Separations. *Chem. Rev.* **2012**, *112*, 869–932. [CrossRef] [PubMed]
19. Kreno, L.E.; Leong, K.; Farha, O.K.; Allendorf, M.; van Duyne, R.P.; Hupp, J.T. Metal–Organic Framework Materials as Chemical Sensors. *Chem. Rev.* **2011**, *112*, 1105–1125. [CrossRef] [PubMed]
20. Wu, H.H.; Gong, Q.H.; Olson, D.H.; Li, J. Commensurate Adsorption of Hydrocarbons and Alcohols in Microporous Metal Organic Frameworks. *Chem. Rev.* **2012**, *112*, 836–868. [CrossRef] [PubMed]
21. Kizzie, A.C.; Wong-Foy, A.G.; Matzger, A.J. Effect of Humidity on the Performance of Microporous Coordination Polymers as Adsorbents for CO_2 Capture. *Langmuir* **2011**, *27*, 6368–6373. [CrossRef] [PubMed]
22. Dietzel, P.D.C.; Johnsen, R.E.; Fjellvag, H.; Bordiga, S.; Groppo, E.; Chavan, S.; Blom, R. Adsorption properties and structure of CO_2 adsorbed on open coordination sites of metal-organic framework Ni2(dhtp) from gas adsorption, IR spectroscopy and X-ray diffraction. *Chem. Commun.* **2008**, *0*, 5125–5127. [CrossRef] [PubMed]
23. Wu, H.; Zhou, W.; Yildirim, T. High-Capacity Methane Storage in Metal Organic Frameworks M_2(dhtp): The Important Role of Open Metal Sites. *J. Am. Chem. Soc.* **2009**, *131*, 4995–5000. [CrossRef] [PubMed]
24. Liu, Y.; Kabbour, H.; Brown, C.M.; Neumann, D.A.; Ahn, C.C. Increasing the Density of Adsorbed Hydrogen with Coordinatively Unsaturated Metal Centers in Metal Organic Frameworks. *Langmuir* **2008**, *24*, 4772–4777. [CrossRef] [PubMed]
25. Bloch, E.D.; Hudson, M.R.; Mason, J.A.; Chavan, S.; Crocellà, V.; Howe, J.D.; Lee, K.; Dzubak, A.L.; Queen, W.L.; Zadrozny, J.M. Reversible CO Binding Enables Tunable CO/H_2 and CO/N_2 Separations in Metal–Organic Frameworks with Exposed Divalent Metal Cations. *J. Am. Chem. Soc.* **2014**, *136*, 10752–10761. [CrossRef] [PubMed]
26. Bonino, F.; Chavan, S.; Vitillo, J.G.; Groppo, E.; Agostini, G.; Lamberti, C.; Dietzel, P.D.; Prestipino, C.; Bordiga, S. Local Structure of CPO-27-Ni Metallorganic Framework upon Dehydration and Coordination of NO. *Chem. Mater.* **2008**, *20*, 4957–4968. [CrossRef]
27. Canepa, P.; Arter, C.A.; Conwill, E.M.; Johnson, D.H.; Shoemaker, B.A.; Soliman, K.Z.; Thonhauser, T. High-throughput screening of small-molecule adsorption in MOF. *J. Mater. Chem. A* **2013**, *1*, 13597–13604. [CrossRef]

28. Tan, K.; Zuluaga, S.; Fuentes, E.; Mattson, E.C.; Veyan, J.-F.; Wang, H.; Li, J.; Thonhauser, T.; Chabal, Y.J. Trapping gases in metal organic frameworks with a selective surface molecular barrier layer. *Nat. Commun.* **2016**, *7*, 13871–13879. [CrossRef] [PubMed]
29. Tan, K.; Zuluaga, S.; Gong, Q.; Gao, Y.; Nijem, N.; Li, J.; Thonhauser, T.; Chabal, Y.J. Competitive Coadsorption of CO_2 with H_2O, NH_3, SO_2, NO, NO_2, N_2, O_2, and CH_4 in M-MOF-74 (M = Mg, Co, Ni): The Role of Hydrogen Bonding. *Chem. Mater.* **2015**, *27*, 2203–2217. [CrossRef]
30. Zuluaga, S.; Fuentes-Fernandez, E.M.A.; Tan, K.; Arter, C.A.; Li, J.; Chabal, Y.J.; Thonhauser, T. Chemistry in confined spaces: Reactivity of the Zn-MOF-74 channels. *J. Mater. Chem. A* **2016**, *4*, 13176–13182. [CrossRef]
31. Zuluaga, S.; Fuentes-Fernandez, E.M.A.; Tan, K.; Xu, F.; Li, J.; Chabal, Y.J.; Thonhauser, T. Understanding and controlling water stability of MOF-74. *J. Mater. Chem. A* **2016**, *4*, 5176–5183. [CrossRef]
32. Kresse, G.; Furthmüller, J. Efficient iterative schemes for ab initio total-energy calculations using a plane-wave basis set. *Phys. Rev. B* **1996**, *54*, 1169–1186. [CrossRef]
33. Kresse, G.; Joubert, D. From ultrasoft pseudopotentials to the projector augmented-wave method. *Phys. Rev. B* **1999**, *59*, 1758–1775. [CrossRef]
34. Berland, K.; Cooper, V.R.; Lee, K.; Schröder, E.; Thonhauser, T.; Hyldgaard, P.; Lundqvist, B.I. van der Waals forces in density functional theory: A review of the vdW-DF method. *Rep. Prog. Phys.* **2015**, *78*, 066501. [CrossRef] [PubMed]
35. Langreth, D.; Lundqvist, B.I.; Chakarova-Käck, S.D.; Cooper, V.; Dion, M.; Hyldgaard, P.; Kelkkanen, A.; Kleis, J.; Kong, L.; Li, S. A density functional for sparse matter. *J. Phys. Condens. Matter* **2009**, *21*, 084203. [CrossRef] [PubMed]
36. Thonhauser, T.; Cooper, V.R.; Li, S.; Puzder, A.; Hyldgaard, P.; Langreth, D.C. Van der Waals density functional: Self-consistent potential and the nature of the van der Waals bond. *Phys. Rev. B* **2007**, *76*, 125112. [CrossRef]
37. Thonhauser, T.; Zuluaga, S.; Arter, C.; Berland, K.; Schröder, E.; Hyldgaard, P. Spin Signature of Nonlocal Correlation Binding in Metal-Organic Frameworks. *Phys. Rev. B* **2015**, *115*, 136402. [CrossRef] [PubMed]
38. Henkelman, G.; Uberuaga, B.P.; Jonsson, H. A climbing image nudged elastic band method for finding saddle points and minimum energy paths. *J. Chem. Phys.* **2000**, *113*, 9901–9904. [CrossRef]
39. Henkelman, G.; Jónsson, H. Improved tangent estimate in the nudged elastic band method for finding minimum energy paths and saddle points. *J. Chem. Phys.* **2000**, *113*, 9978–9985. [CrossRef]
40. Falk, M.; Whalley, E. Infrared Spectra of Methanol and Deuterated Methanols in Gas, Liquid, and Solid Phases. *J. Chem. Phys.* **1961**, *34*, 1554–1568. [CrossRef]
41. Canepa, P.; Hanson, R.M.; Ugliengo, P.; Alfredsson, M. J-ICE: A new Jmol interface for handling and visualizing crystallographic and electronic properties. *J. Appl. Crystallogr.* **2011**, *44*, 225–229. [CrossRef]
42. Li, Y.; Wang, X.; Xu, D.; Chung, J.D.; Kaviany, M.; Huang, B. H_2O Adsorption/Desorption in MOF-74: Ab Initio Molecular Dynamics and Experiments. *J. Phys. Chem. C* **2015**, *119*, 13021–13031. [CrossRef]